Evidence For Neutrino Oscillations at LSND

Eric D. Church
University of California, Riverside, CA 92521
echurch@lanl.gov,

representing the LSND collaboration.

Searches for $\nu_\mu \rightarrow \nu_e$ [1] and $\overline{\nu}_\mu \rightarrow \overline{\nu}_e$ [2] oscillations with the LSND experiment [3] at the Los Alamos Meson Physics Facility have been performed using ν_μ from π^+ decay in flight (DIF) and $\overline{\nu}_\mu$ from μ^+ decay at rest (DAR), respectively. The 1993-95 DIF (1993-98 **preliminary** DAR) analysis finds an oscillation probability of $(2.6 \pm 1.0) \times 10^{-3}$ ($(3.3 \pm 1.0) \times 10^{-3}$), with a probability of statistical fluctuation equal to $\sim 1.1 \times 10^{-3}$ ($\sim 4.1 \times 10^{-8}$). The most-favored Δm^2 range, taking into account results at all experiments, is $0.2 \lesssim \Delta m^2 \lesssim 2$ eV^2.

I. INTRODUCTION

The main source of DIF (DAR) ν_μ ($\overline{\nu}_\mu$) for this experiment is the A6 water target of the LAMPF 800 MeV proton linear accelerator. Approximately 3.4% of the π^+ produced in the 30 cm target decay in flight before reaching the water-cooled copper beam stop, roughly 1.5m downstream, to give the DIF flux. The remainder of the π^+ decay at rest to μ^+, nearly all of which decay at rest to give the DAR flux. Two upstream thin carbon targets, A1 and A2, located 135m and 110 m upstream from the detector center, respectively, provide additional small contributions to the fluxes, which may be significant for the DIF analysis if Δm^2 is small, due the long baselines. The LSND measurement [4] of the exclusive reaction $\mu^{-12}\mathrm{N}_{g.s.}$, with its well-understood cross section, confirms the DIF flux to within a 15% error, while the LSND measurements [5] of the $\nu_e C$ and $\nu_e e$ elastic cross sections fix the DAR flux to within a smaller error. [4] and [5] show excellent agreement between the LSND results and the theoretical expectations for these cross-sections.

The data taken for the two analyses reported here comes from runs taken in 1993, 1994 and 1995, with total charges delivered to the beam stop of 1787 C, 5904 C and 7081 C. Preliminary results for the DAR analysis from an extra 13970 C in the 1996-1998 data are also shown.

The detector is a tank filled with 167 metric tons of dilute liquid scintillator, located 30m downstream from the neutrino source and surrounded on all sides except the bottom by a liquid scintillator veto shield. The dilute mixture allows detection in the surrounding 1220 tank photomultiplier tubes of both Čerenkov light and scintillation light, so that reconstruction provides robust particle identification (PID) for $e^\pm$, as well as the direction and position of the $e^\pm$.

Despite 2.0 kg/cm^2 shielding above the detector tunnel, there remains a large background to the oscillation search due to cosmic rays. The background is highly suppressed by a veto shield [6] which provides active and passive shielding. If six or more of the 292 veto tubes fired in one 100 nsec interval, a signal holds off the trigger for 15.2 μsec. An 18% cost in dead-time is incurred due to the veto hold-off, while a veto inefficiency of $< 10^{-5}$ is achieved off-line for incident charged particles. The veto inefficiency is much larger for incident cosmic-ray neutrons.

The data acquisition and triggering do not depend on whether the beam is on or off, thus the beam-on to beam-off duty ratio can be measured for triggered events; it averaged 0.070 ± 0.001 over 1993-1995. The beam-unrelated background in any beam-on sample is thus well measured from the much larger beam-off sample and can be subtracted. Still, the cuts used to select $e^\pm$ in the two analyses are designed to discriminate heavily against this background so that the statistical error from the subtraction may be kept small relative to the beam-dependent signal.

II. ANALYSIS: DAR

A DAR oscillation event signature consists of an "electron" signal followed by a 2.2 MeV photon correlated with the electron in both position and time. Detection of DAR ν_e is dominated in LSND by charge current reactions on

^{12}C. However, electrons from $\nu_e^{12}C \to e^{-\,12}N$ have energy $E_e < 36$ MeV. Moreover, DAR production of a correlated photon from $\nu_e^{12}C \to e^- n^{11}N$ can only occur for $E_e < 20$ MeV. These properties of the $\nu_e^{12}C$ background are exploited in our energy selection cuts.

PID in the DAR analysis is achieved in a straightforward way [2] which exploits the differences in the position, timing and angle distributions in events with particles above and below Čerenkov threshold. See figure 1.

Separation of correlated neutron-capture photons from the accidental signals is achieved using an approximate likelihood ratio R [7,2] for the correlated and accidental hypotheses. R discriminates between correlated and accidental photons by exploiting the quite-different distributions in three variables: the time and distance between the reconstructed photon and $e^{\pm}$ vertices and the tank hit multiplicity distribution of the photon.

Figure 2 shows the R distribution for the $e^{12}N_{g.s.}$ sample in which one expects there to be no correlated photon (since no neutron is produced in the reaction), and the facing figure shows the **preliminary** 1993-98 DAR R distribution. The first plot in figure 2 shows that a sample of entirely accidental gammas indeed fits the accidental gamma R shape, leaving no room for a contribution from correlated gammas. From the second plot one obtains the number of events in the DAR sample which have correlated gammas and which thus satisfy the conditions to be oscillation signature events. This is one way in which one may count oscillation events. The other is to simply cut at a large value of R, above which one has a high purity oscillation candidate sample, and count the events which survive. We do the former to calculate the oscillation probability in order to take advantage of the bigger efficiency, while the latter sample may be used for the purpose of making distributions of energy, position, etc.

Figure 3 shows the **preliminary** energy distribution of the $e^{\pm}$ sample with $R > 30$ using all of the data from 1993-1998.

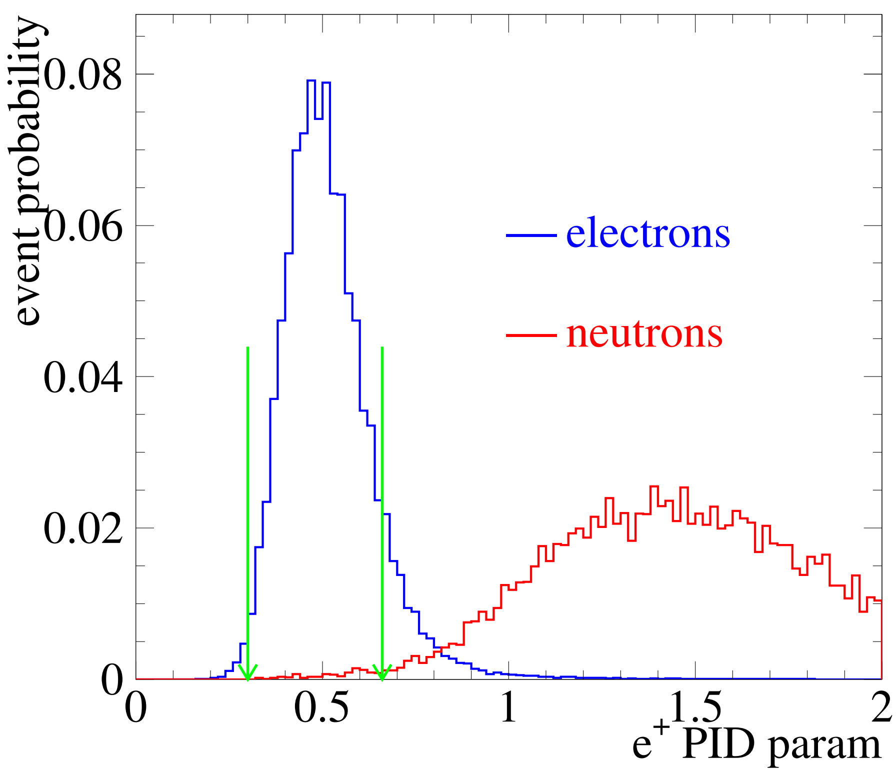

FIG. 1. Particle ID parameter for electrons and neutrons. The arrows indicate the positions of the cuts for this analysis.

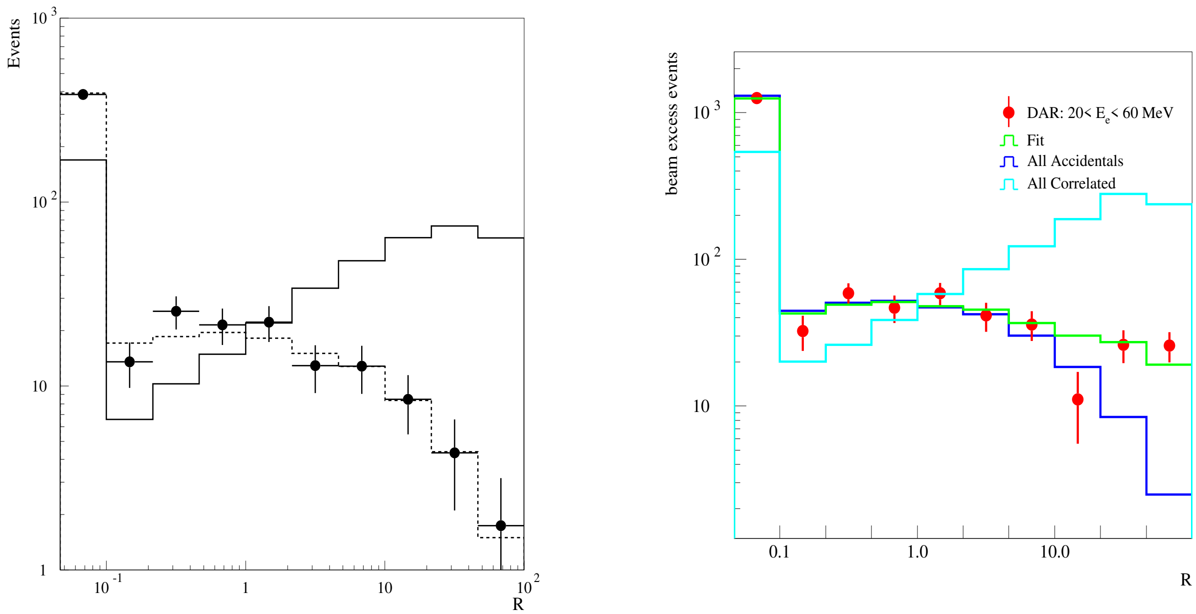

FIG. 2. The R distribution for the $e^{12}N_{g.s.}$ sample is on the left. In this plot the dashed histogram is the distribution if the γs are taken to be entirely uncorrelated, and the solid is the distribution if the γs are taken to be entirely correlated. The **preliminary** 1993-98 R distribution for the DAR sample is shown on the right.

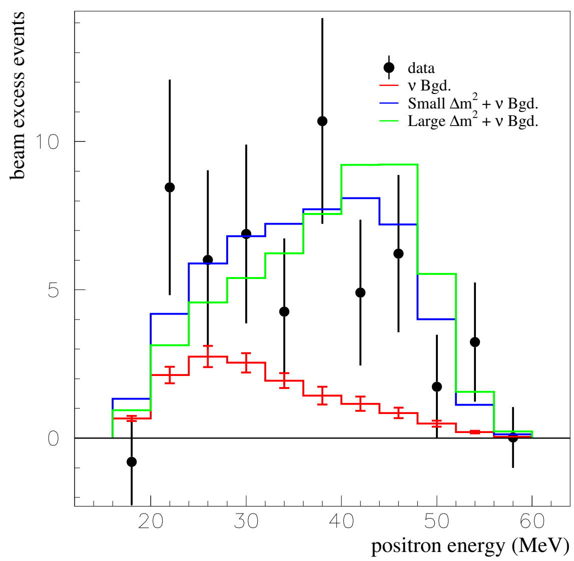

FIG. 3. The **preliminary** 1993-98 beam excess e^+ energy distribution for events with $R > 30$. Shown is the estimated neutrino background, and expected distribution for neutrino oscillations at large and small δm^2 plus estimated neutrino background.

III. ANALYSIS: DIF

The long-track e^- which is produced in the tank from the higher energy ν_e flux requires a more robust PID algorithm than required in the DAR analysis. Such ID is provided by a likelihood technique, in which the measured time and charge on each tube in a selected event is compared against its predicted time and charge. The most likely configuration – vertex, direction and scintillation and Čerenkov strengths of each postulated electron – with respect to the measured quantities is calculated by maximizing the event likelihood among all possible configurations.

The likelihood value of the event itself, as well as quantities such as the ratio in the event of Čerenkov to scintillation light, provide discrimination against electromagnetic background, while other event variables, such as extrapolated track distance back to the tank wall provides discrimination against non-electromagnetic backgrounds, such as π^0s and ns from cosmic-ray induced activity entering the tank. See figure 4.

The energy distribution for the finale sample of events is seen in figure 5.

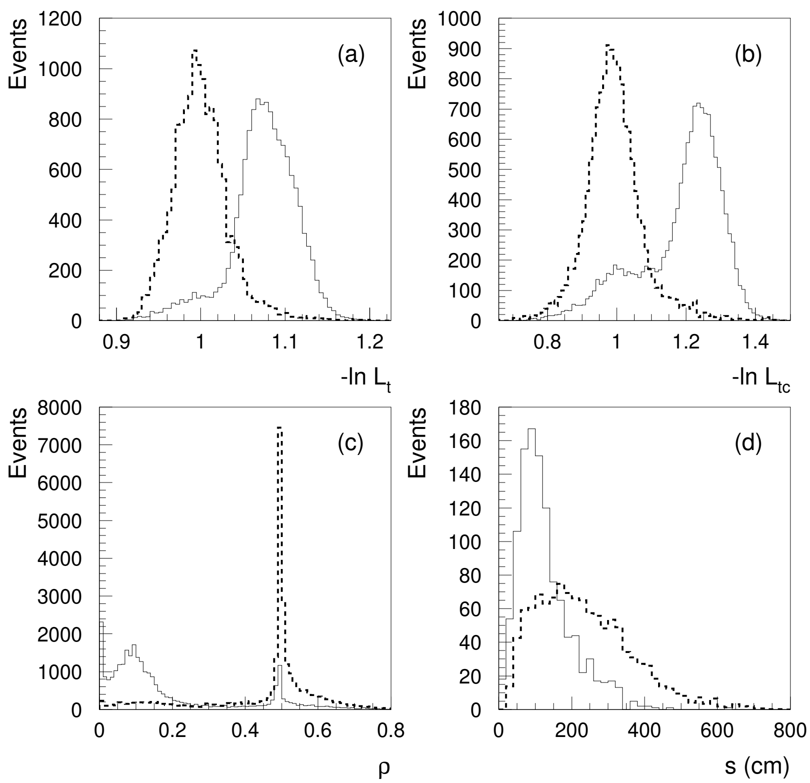

FIG. 4. Timing likelihoods for (a) the entire event and (b) the Čerenkov region only. (c) is the Čerenkov-to-scintillation density ratio, ρ, while (d) is the projected track-length to the tank wall. (a)-(c) correspond to all (beam on+off) DIF data after some pre-selection [1], while (d) corresponds to this same event sample but after all other cuts were applied. Solid is data, dashed is MC normalized to the same area.

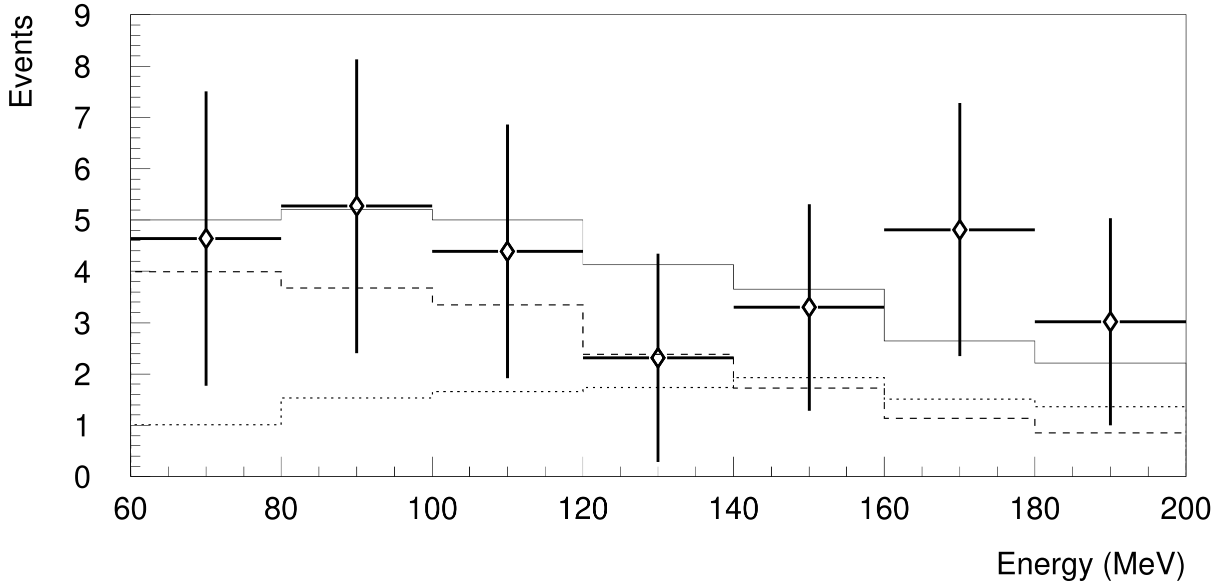

FIG. 5. The energy distribution (points with error bars) for the final beam-excess DIF events. The expectation for backgrounds (dotted histogram), the oscillation signal for large values of δm^2 (dashed histogram) and the some of the two (solid histogram) are shown also.

IV. RESULTS

A 99% likelihood allowed region (DAR analysis) is shown in figure 6 compared with the 95% confidence region from the DIF analysis. The DIF and DAR analyses give consistent allowed regions and oscillation probabilities. Table I shows the results of the DIF and DAR analyses. Papers providing further details on these two analyses may be found at [8].

LSND took its last data in December, 1998.

A global analysis in which both the DAR and DIF νs are treated with the same fitting algorithm and in which all the data from 1993-1998 is included is underway.

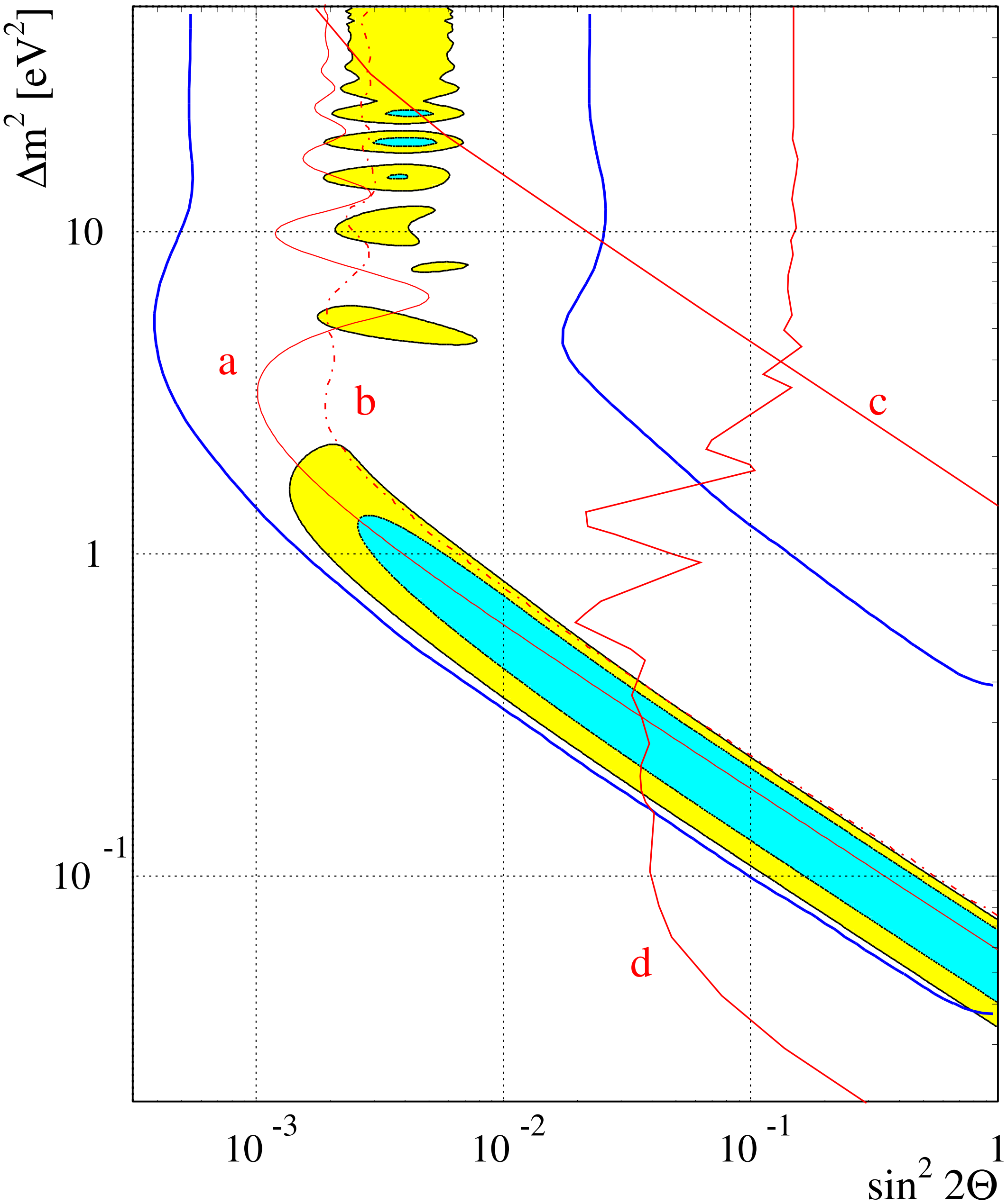

FIG. 6. The allowed regions in $\sin^2\theta - \Delta m^2$ from the LSND DAR analysis are light shaded (4.6 likelihood units down from the maximum) and dark shaded (2.3 likelihood units down from the maximum). The 90% confidence allowed region from the LSND DIF analysis is bounded by the bold lines which enclose the DAR region. The other experiments are as follows: (a) is the 90% exclusion region placed by Karmen II data February, 1997 through November, 1998. (b) is BNL E776, (c) is CCFR, and (d) is Bugey.

TABLE I. Results of the analyses. In the case of the DIF analysis results from the sample corresponding to the logical OR [1] are shown. The DAR results are **preliminary**. The total number of beam on events, background, Excess, and the oscillation probability are shown.

Data	Beam on	Bgd.	Excess	osc'n. prob. (%)
DIF, "OR"	40	21.9 ± 2.1	18.1 ± 6.6	0.26 ± 0.10
DAR, $20 < E_{e^+} < 60$ MeV, $R > 30$	70	30.5 ± 1.8	39.5 ± 8.8	0.33 ± 0.10

[1] C. Athanassopoulos *et al.* (LSND Collaboration), Phys. Rev. **C58** 2489 (1998).
C. Athanassopoulos *et al.* (LSND Collaboration), Phys. Rev. Lett. **81** 1774 (1998).

[2] C. Athanassopoulos *et al.* (LSND Collaboration), Phys. Rev. **C54** 2685 (1996).
C. Athanassopoulos *et al.* (LSND Collaboration), Phys. Rev. Lett. **77** 3082 (1996).

[3] C. Athanassopoulos, *et. al.*, Nucl. Inst. and Meth. A **388** 149 (1997).

[4] C. Athanassopoulos *et al.* (LSND Collaboration), Phys.Rev. **C56** 2806 (1997).

[5] C. Athanassopoulos *et al.* (LSND Collaboration), Phys. Rev. C **55,** 2078 (1997).
N. Wadia, PhD. Thesis, Louisiana State University (1998).

[6] J. J. Napolitano *et. al.*, Nucl. Inst. and Meth. A **388** 149 (1997).

[7] C. Athanassopoulos *et al.* (LSND Collaboration), Phys. Rev. Lett. **75**, 2650 (1995).

[8] *http://www.neutrino.lanl.gov.*